

# MODELING AND CONTROL OF CENTRALIZED EVS FOR REGULATION SERVICE

Mingshen Wang<sup>1</sup>, Yunfei Mu<sup>1\*</sup>, Hongjie jia<sup>1</sup>, Wenjin Qi<sup>2</sup>, Qian jiang<sup>1</sup>, Xiaolong jin<sup>1</sup>

1 Key Laboratory of Smart Grid of Ministry of Education of Tianjin University, Tianjin 300072, China

2 Jiangsu Electric Power Design Institute, Nanjing 211102, China

## ABSTRACT

The high penetration of renewable energy incurs serious power fluctuations in the power system. The electric vehicles (EVs) under the centralized control tend to provide considerable regulation capacity for the power system. In the existing modeling methods for centralized EVs, the accurate control results for the regulation services were achieved by modeling each EV individually. However, the computational complexity was a serious problem for modeling large scale EVs. In this paper, a reduced modeling method for centralized EVs is developed by describing a population of EVs with a partial differential equation (PDE). This PDE modeling method uses a finite number of state-of-charge (SOC) intervals to describe the flows of charging, idle and discharging EVs. Considering the three connecting states (CNS) of EVs, this PDE modeling method realizes the power regulation for centralized EVs by changing the CNS of EVs located in different SOC intervals. Comparative simulations validate that the PDE modeling method for large scale centralized EVs achieves high control accuracy and high computational efficiency.

**Keywords:** electric vehicle (EV), centralized control, regulation service, partial differential equation (PDE)

## 1. INTRODUCTION

The stochastic characteristics of renewable energy add the difficulty to the power system regulation. In recent years, the electric vehicle (EV) has aroused considerable attention for its energy-saving feature and low-carbon emission. Large scale EVs under the centralized control have the potential to provide the effective regulation service for the power system [1].

After travel, an EV requires connecting to the power

grid and charge enough energy for its future travel. For an individual EV, the connecting period is usually much longer than the required charging period. Thus, we can change the EV's power exchange with the power grid for the regulation service during the connecting period. Though the regulation capacity of one EV is small, the total regulation capacity of large scale EVs is considerable. It is essential to develop an effective modeling method for large scale EVs under the centralized control.

A number of modeling methods have been conducted to implement the power regulation for centralized EVs. The modeling method for centralized EVs in [2] analyzes the stochastic traveling behaviors of EVs. In [3], the modeling for centralized EVs considers the various vehicle types. In [4], the various charging modes are considered in the modeling process for centralized EVs. The regulation for centralized EVs is realized by generating the individual control signal for each EV [5]. These modeling methods need to feature each EV and are regarded as the individual modeling method. However, the stochastic traveling behaviors, the various vehicle types, and the different charging modes incurred the different response characteristics of EVs and increased the computational complexity for modeling large scale EVs. For regulating large scale EVs, the numerous individual control signals added the control difficulty for centralized EVs as transmitting so many individual signals at the same time is a heavy workload.

To address these crucial issues, the partial differential equation (PDE) modeling method is used to realize the power regulation for centralized EVs. Firstly, we use PDEs to model individual EVs with three connecting states (CNS), and four responding modes are defined by changing between different CNS. Then based on the respond modes, the EV flows of centralized EVs

are analyzed between the divided state-of-charge (SOC) intervals with a finite number, and the EV flows under different CNS are modeled with the PDEs. Considering the traveling behaviors of EVs, we use a unified PDE to describe the EV flows for EVs with different CNS. The modeling complexity is significantly decreased as the number of SOC intervals can be much smaller than the number of EVs. Then, the power regulation for centralized EVs is realized by computing the proportion of controlled EVs in each SOC interval, which simplifies the control process for large scale centralized EVs. Compared with the individual modeling method, simulation results validate the effectiveness of the PDE modeling and control method for centralized EVs.

## 2. MODELING FOR AN INDIVIDUAL EV

After travel, an EV requires connecting to the power system and withdraws enough energy for its future travel. Based on the power flow directions, the CNS of an EV can be divided into the charging state (CS), the idle state (IS), and the discharging state (DS). During the connecting period, the SOC variations of an EV can be described by the partial differential equation (PDE) as given by (1).

$$\dot{s}_i(t) = \begin{cases} p_{i,cs} \cdot \eta_{i,cs} / q_i, & \text{CS} \\ 0, & \text{IS} \\ -p_{i,ds} / \eta_{i,ds} / q_i, & \text{DS} \end{cases} \quad (1)$$

where  $i$  is the index of EVs;  $s_i(t)$  is the SOC value at time  $t$ ;  $q_i$  is the battery capacity;  $p_{i,cs}/p_{i,ds}$  is the rated charging/discharging (C/D) power, respectively; and  $\eta_{i,cs}/\eta_{i,ds}$  is the C/D efficiency.

Based on the three CNS, four responding modes (RMs) are defined by changing from one CNS to another: (i) 'CS→IS', (ii) 'IS→DS', (iii) 'DS→IS', and (iv) 'IS→CS'.

## 3. MODELING AND CONTROL FOR CENTRALIZED EVS

### 3.1 PDE modeling for centralized EVs

For a population of system-connected EVs,  $X_{cs}(t,s)$ ,  $X_{is}(t,s)$ , and  $X_{ds}(t,s)$  are defined as the numbers of EVs at SOC  $s$  and time  $t$ , with the CNS of CS, IS, and DS, respectively. Taking the EVs in CS as the example, the flow of EVs represented by  $X_{cs}(s,t)$  crossing SOC  $s$  can be described by (2).

$$F_{cs}(t,s) = X_{cs}(t,s) \cdot [ds/dt] \quad (2)$$

where  $[ds/dt]$  indicates the average SOC variation of EVs in CS with respect to time.

Based on Eq. (1), Eq. (2) is further described by (3).

$$F_{cs}(t,s) = X_{cs}(t,s) \cdot [p_{cs} \cdot \eta_{cs} / q] \quad (3)$$

where  $p_{cs}$ ,  $\eta_{cs}$ , and  $q$  are the homogeneous parameters of  $p_{i,cs}$ ,  $\eta_{i,cs}$ , and  $q_i$ , respectively.

Within an infinitesimal SOC interval  $[s, s+ds]$ , the variation of  $X_{cs}(s,t)$  with respect to time is achieved by the difference between the entering flow and the existing flow as given by (4).

$$\begin{aligned} \partial X_{cs}(t,s) / \partial t &= \lim_{ds \rightarrow 0} [(F_{cs}(t,s) - F_{cs}(t,s+ds)) / ds] \\ &= -\partial F_{cs}(t,s) / \partial s = -a_{cs} \cdot \partial X_{cs}(t,s) / \partial s \end{aligned} \quad (4)$$

where  $a_{cs} = p_{cs} \cdot \eta_{cs} / c$ .

For the EVs in IS and DS, the variations of  $X_{is}(s,t)$  and  $X_{ds}(s,t)$  with respect to time can be similarly achieved by (5) and (6), respectively.

$$\partial X_{is}(t,s) / \partial t = 0 \quad (5)$$

$$\partial X_{ds}(t,s) / \partial t = -a_{ds} \cdot \partial X_{ds}(t,s) / \partial s \quad (6)$$

where  $a_{ds} = -p_{ds} / \eta_{ds} / c$ .

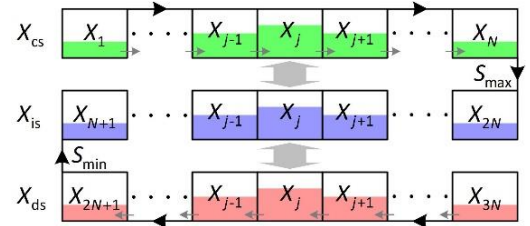


Fig 1 SOC intervals and EV flows

As given by Fig. 1, EVs' SOC variation range  $[S_{min}, S_{max}]$  is divided into  $N$  small SOC intervals. For the EVs in CS and DS, the EV flow between two adjacent SOC intervals is illustrated by an arrow. Considering RMs 'CS→IS' and 'IS→CS', the EV flows of EVs in CS are described by (7) based on Eq. (4). Considering RMs 'DS→IS' and 'IS→DS', the flows of EVs in DS are described by (8) based on Eq. (6). Considering all the four RMs, the EV flows of EVs in IS are described by (9) based on Eq. (5).

$$\begin{cases} \dot{X}_1(t) = -a_{cs} / \Delta s \cdot X_1(t) \cdot u_1(t) \cdot X_1(t) + v_{1+N}(t) \cdot X_{1+N}(t) \\ \dot{X}_j(t) = -a_{cs} / \Delta s \cdot (X_j(t) - X_{j-1}(t)) \\ \quad - u_j(t) \cdot X_j(t) + v_{j+N}(t) \cdot X_{j+N}(t), \quad 2 \leq j \leq N \end{cases} \quad (7)$$

where  $\Delta s = (S_{min} - S_{max}) / N$ ;  $X_j$  represents the number of EVs located in SOC interval  $j$ ;  $u_j(t)$  ( $1 \leq j \leq N$ ) represents the proportion of EVs in  $X_j$  for the 'CS→IS' control; and  $v_j(t)$  ( $N+1 \leq j \leq 2N$ ) represents the proportion of EVs in  $X_j$  for the 'IS→CS' control and  $v_j(t) = 0$  ( $1 \leq j \leq N$ ).

$$\begin{cases} \dot{X}_j(t) = -a_{ds} / \Delta s \cdot (X_{j+1}(t) - X_j(t)) \\ \quad + u_{j-N}(t) \cdot X_{j-N}(t) - v_j(t) \cdot X_j(t), \quad 2N+1 \leq j \leq 3N-1 \\ \dot{X}_{3N}(t) = a_{ds} / \Delta s \cdot X_{3N}(t) + u_{2N}(t) \cdot X_{2N}(t) - v_{3N}(t) \cdot X_{3N}(t) \end{cases} \quad (8)$$

where  $u_j(t)$  ( $N+1 \leq j \leq 2N$ ) represents the proportion of EVs in  $X_j$  for the 'IS→DS' control and  $u_j(t) = 0$  ( $2N+1 \leq j \leq 3N$ ); and  $v_j(t)$  ( $2N+1 \leq j \leq 3N$ ) represents the proportion of EVs in  $X_j$  for the 'DS→IS' control.

$$\begin{cases} \dot{X}_{2N}(t) = a_{cs} / \Delta s \cdot X_N(t) + u_N(t) \cdot X_N(t) - v_{2N}(t) \cdot X_{2N}(t) \\ \quad - u_{2N}(t) \cdot X_{2N}(t) + v_{3N}(t) \cdot X_{3N}(t) \\ \dot{X}_j(t) = u_{j-N}(t) \cdot X_{j-N}(t) - v_j(t) \cdot X_j(t) \\ \quad - u_j(t) \cdot X_j(t) + v_{N+j}(t) \cdot X_{N+j}(t), \quad N+2 \leq j \leq 2N-1 \\ \dot{X}_{N+1}(t) = -a_{ds} / \Delta s \cdot X_{2N+1}(t) + u_1(t) \cdot X_1(t) - v_{N+1}(t) \cdot X_{N+1}(t) \\ \quad - u_{N+1}(t) \cdot X_{N+1}(t) + v_{2N+1}(t) \cdot X_{2N+1}(t) \end{cases} \quad (9)$$

Based on Eq. (7), Eq. (8), and Eq. (9), the EV flows of EVs in CS, IS, and DS are described by a unified PDE as given by (10).

$$\dot{\mathbf{X}}(t) = \mathbf{A} \cdot \mathbf{X}(t) + (\mathbf{B} \cdot \mathbf{U}(t) + \mathbf{C} \cdot \mathbf{V}(t)) \cdot \mathbf{X}(t) \quad (10)$$

where  $\mathbf{X}(t) = [X_1(t), \dots, X_{3N}(t)]^T$ ;  $\mathbf{U}(t) = \text{diag}([u_1(t), \dots, u_{3N}(t)])$ ;  $\mathbf{V}(t) = \text{diag}([v_1(t), \dots, v_{3N}(t)])$ ;  $\mathbf{A}$  is a  $(3N \times 3N)$  sparse constant matrix as given by (11); and both  $\mathbf{B}$  and  $\mathbf{C}$  are  $(3N \times 3N)$  constant matrices as given by (12).

$$\begin{cases} A_{1,1} = -\pi_{cs}, A_{j,j-1} = \pi_{cs}, A_{j,j} = -\pi_{cs}; \quad 2 \leq j \leq N \\ A_{N+1,2N+1} = -\pi_{ds}, A_{2N,N} = \pi_{cs}; \\ A_{j,j} = \pi_{ds}, A_{j,j+1} = -\pi_{ds}, A_{3N,3N} = \pi_{ds}; \quad 2N+1 \leq j \leq 3N-1 \end{cases} \quad (11)$$

where  $\pi_{cs} = a_{cs} / \Delta s$ ; and  $\pi_{ds} = a_{ds} / \Delta s$ .

$$\mathbf{B} = \begin{bmatrix} -\mathbf{I}_{N \times N} & \mathbf{0}_{N \times N} & \mathbf{0}_{N \times N} \\ \mathbf{I}_{N \times N} & -\mathbf{I}_{N \times N} & \mathbf{0}_{N \times N} \\ \mathbf{0}_{N \times N} & \mathbf{I}_{N \times N} & \mathbf{0}_{N \times N} \end{bmatrix}, \quad \mathbf{C} = \begin{bmatrix} \mathbf{0}_{N \times N} & \mathbf{I}_{N \times N} & \mathbf{0}_{N \times N} \\ \mathbf{0}_{N \times N} & -\mathbf{I}_{N \times N} & \mathbf{I}_{N \times N} \\ \mathbf{0}_{N \times N} & \mathbf{0}_{N \times N} & -\mathbf{I}_{N \times N} \end{bmatrix} \quad (12)$$

where  $\mathbf{I}_{N \times N}$  represents the  $(N \times N)$  identity matrix; and  $\mathbf{0}_{N \times N}$  represents the  $(N \times N)$  zero matrix.

The dynamic plugging in and out have a direct impact on the EV flows as given by (13).

$$\mathbf{X}_p(t) = N_{in} \cdot f_{in}(t) \cdot \mathbf{X}_{in} - N_{out} \cdot f_{out}(t) \cdot \mathbf{X}_{out} \quad (13)$$

where  $f_{in}$  and  $f_{out}$  are the probability density functions of EVs' plugging in and out during a day, respectively;  $N_{in}$  and  $N_{out}$  are the predicted numbers of EVs plugging in and out during a day, respectively; and  $\mathbf{X}_{in}$  and  $\mathbf{X}_{out}$  indicate the EVs' probability distributions among all SOC intervals when an EV plugs in and out, respectively.

Then, the EV flows of centralized EVs are corrected by (14).

$$\dot{\mathbf{X}}(t) = \mathbf{A} \cdot \mathbf{X}(t) + (\mathbf{B} \cdot \mathbf{U}(t) + \mathbf{C} \cdot \mathbf{V}(t)) \cdot \mathbf{X}(t) + \mathbf{X}_p(t) \quad (14)$$

### 3.2 Regulation with PDE Model of EVs

Based on the PDE model of centralized EVs in Eq. (14), we can discrete the PDE model as given by (15). Then, the total power of centralized EVs can be achieved by (16), and the regulation capacity of centralized EVs under different RMs can be achieved by (17).

$$\mathbf{X}(t+\Delta t) = (\mathbf{A} \cdot \Delta t + \mathbf{I}) \cdot \mathbf{X}(t) + (\mathbf{B} \cdot \mathbf{U}(t) + \mathbf{C} \cdot \mathbf{V}(t)) \cdot \Delta t \cdot \mathbf{X}(t) + \mathbf{X}_p(t) \cdot \Delta t \quad (15)$$

$$P_{ev}(t) = \mathbf{E} \cdot \mathbf{X}(t) \quad (16)$$

where  $\mathbf{E} = [p_{cs} \cdot \mathbf{1}_{1 \times N}, \mathbf{0}_{1 \times N}, -p_{ds} \cdot \mathbf{1}_{1 \times N}]$ .

$$\begin{cases} P_{c2i}(t) = \mathbf{D}_{c2i} \cdot \mathbf{X}(t), \quad P_{i2d}(t) = \mathbf{D}_{i2d} \cdot \mathbf{X}(t) \\ P_{d2i}(t) = \mathbf{D}_{d2i} \cdot \mathbf{X}(t), \quad P_{i2c}(t) = \mathbf{D}_{i2c} \cdot \mathbf{X}(t) \end{cases} \quad (17)$$

where  $P_{c2i}$ ,  $P_{i2d}$ ,  $P_{d2i}$ , and  $P_{i2c}$  are the regulation capacity of centralized EVs under 'CS  $\rightarrow$  IS', 'IS  $\rightarrow$  DS', 'DS  $\rightarrow$  IS', and 'IS  $\rightarrow$  CS', respectively;  $\mathbf{D}_{c2i} = [-p_{cs} \cdot \mathbf{1}_{1 \times N}, \mathbf{0}_{1 \times 2N}]$ ;  $\mathbf{D}_{i2d} = [-p_{ds} \cdot \mathbf{1}_{1 \times 2N}, \mathbf{0}_{1 \times N}]$ ;  $\mathbf{D}_{d2i} = [\mathbf{0}_{1 \times 2N}, p_{ds} \cdot \mathbf{1}_{1 \times N}]$ ; and  $\mathbf{D}_{i2c} = [\mathbf{0}_{1 \times N}, p_{cs} \cdot \mathbf{1}_{1 \times 2N}]$ .

$P^*(t)$  is defined as the target regulation power of centralized EVs. Then, we tends to transform  $P^*(t)$  into  $\mathbf{U}(t)$  and  $\mathbf{V}(t)$  and predict  $\mathbf{X}(t+\Delta t)$  for centralized EVs. When  $P^*(t) < 0$ ,  $\mathbf{U}(t)$  is determined by (17) with the SOC sorting method and  $\mathbf{V}(t) = \mathbf{0}$ ; and thus EVs with the lower SOC are more likely to be controlled for power increase. When  $P^*(t) > 0$ ,  $\mathbf{U}(t) = \mathbf{0}$  and  $\mathbf{V}(t)$  is determined by (18) with the SOC sorting method; and thus EVs with the higher SOC are more likely to be controlled for power decrease.

$$\begin{cases} X^* = \max(P^*(t), P_{c2i}(t)) / (-p_{cs}) \\ u_j(t) = \min(X^* - X_{j+1:N}(t), X_j(t)) / X_j(t), \quad 1 \leq j \leq N \end{cases} \quad (18a)$$

$$\begin{cases} X^* = \max(P^*(t) - P_{c2i}(t), 0) / (-p_{ds}) \\ u_j(t) = \min(X^* - X_{j+1:2N}(t) - X_{j-N+1:N}(t), X_j(t) + X_{j-N}(t)) \\ \quad / (X_j(t) + X_{j-N}(t)), \quad N+1 \leq j \leq 2N \end{cases} \quad (18b)$$

$$\begin{cases} X^* = \min(P^*(t), P_{d2i}(t)) / p_{ds} \\ u_j(t) = \min(X^* - X_{j+1:3N}(t), X_j(t)) / X_j(t), \quad 2N+1 \leq j \leq 3N \end{cases} \quad (19a)$$

$$\begin{cases} X^* = \max(P^*(t) - P_{d2i}(t), 0) / p_{cs} \\ u_j(t) = \min(X^* - X_{j+1:2N}(t) - X_{j+N+1:3N}(t), X_j(t) + X_{j+N}(t)) \\ \quad / (X_j(t) + X_{j+N}(t)), \quad N+1 \leq j \leq 2N \end{cases} \quad (19b)$$

where  $X_{j:k}$  represents the summation of  $[X_j, \dots, X_k]$ .

## 4. CASE STUDIES AND SIMULATION RESULTS

The distributions of charging and discharging parameters of EVs are shown in Table I [6]. The distributions of traveling parameters of EVs are derived from [7]. The simulations are conducted with MATLAB installed on a laptop with 2.5 GHz i7-4710MQ CUP and 8 GB RAM.

Table I Charging and discharging parameters of EVs

Parameter	Definition	Distribution*
$p_{i,cs}/p_{i,ds}$	Rated C/D power (kW)	F(5,7)
$\eta_{i,cs}/\eta_{i,ds}$	Rated C/D efficiency	F(0.88,0.95)
$q_i$	Battery capacity (kWh)	F(20,30)

\*F( $\alpha, \beta$ ) represents the uniform distribution within  $[\alpha, \beta]$ .

Based on the distributions of EV parameters, the PDE modeling method is used to estimate the regulation

capacity of centralized EVs. Then, the centralized EVs are used to respond to the predefined target regulation power, and  $U(t)$  and  $V(t)$  are determined as the proportion of controlled EVs in each SOC interval.

To verify the PDE modeling method for EVs' control, each EV achieves its parameters from the distributions. Then, each EV is simulated to respond to  $U(t)$  and  $V(t)$  and achieve its regulation capacity individually. Then, the regulation capacity of centralized EVs is obtained by summing the regulation capacity of all EVs. This individual modeling method has been widely used in existing literatures.

The predefined one-hour regulation power profile is shown in Fig. 2 [8]. When the centralized EVs respond to the regulation power profile, the base value for the regulation power profile is 75% the total regulation capacity of centralized EVs. The power profiles of centralized EVs with regulation service are shown in Fig. 3. It is obvious that the PDE modeling method achieves the control result for centralized EVs with high accuracy compared with the individual modeling method.

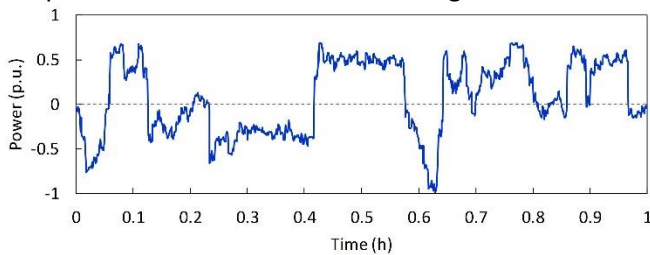


Fig 2 Target regulation power profile with 3600 samples

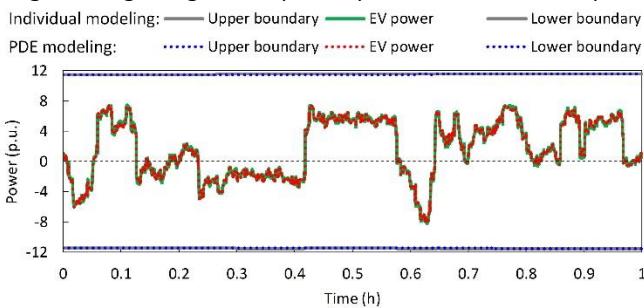


Fig 3 Power profiles of centralized EVs (2,000 EVs and 30 SOC intervals)

Table II Computational time under different EV numbers

EV number	PDE modeling	Individual modeling
500	0.00612 s	3.072 s
1,000	0.00613 s	6.471 s
1,500	0.00611 s	9.636 s
2,000	0.00614 s	12.796 s

Then, the average computational times for each time step are compared under different EV numbers. As shown in Table II, the computational time of the PDE modeling method is much shorter than that of the individual modeling method. With the increase of EV

number, the computational time of the individual modeling method increases significantly. While with the PDE modeling method, the computational time is almost constant to a rather small value.

## 5. CONCLUSIONS

In this paper, a PDE modeling method is developed to estimate the regulation capacity and realize the power regulation service. Comparative simulation results validate that the PDE modeling method can achieve the high control accuracy with the much reduced computational time.

## ACKNOWLEDGEMENT

This work was supported by the National Natural Science Foundation of China (No. U176621, No. 51677124), and the Foundation of China Scholarship Council (No. 201706250184).

## REFERENCE

- [1] Ma Y, Houghton T, Cruden A, Infield D. Modeling the benefits of vehicle-to-grid technology to a power system. *IEEE Trans Power Syst* 2012; 27(2): 1012–20.
- [2] Dallinger D, Krampe D, Wietschel M. Vehicle-to-grid regulation reserves based on a dynamic simulation of mobility behavior. *IEEE Trans Smart Grid* 2011; 2(2): 302–13.
- [3] Mu Y, Wu J, Ekanayake J, Jenkins N, Jia H. Primary frequency response from electric vehicles in the Great Britain power system. *IEEE Trans Smart Grid* 2013; 4(2): 1142–50.
- [4] Lin H, Liu Y, Sun Q, Xiong R, Li H, Wennersten R. The impact of electric vehicle penetration and charging patterns on the management of energy hub – A multi-agent system simulation. *Appl Energy* 2018; 230: 189–06.
- [5] Liu H, Hu Z, Song Y, Wang J, Xie X. Vehicle-to-grid control for supplementary frequency regulation considering charging demands. *IEEE Trans Power Syst* 2012; 27(2): 1012–20.
- [6] Mukherjee J C, Gupta A. Distributed charge scheduling of plug-in electric vehicles using inter-aggregator collaboration. *IEEE Trans Smart Grid* 2017; 8(1): 331–41.
- [7] Yao W, Zhao J, Wen F, Xue Y, Ledwich G. A hierarchical decomposition approach for coordinated dispatch of plug-in electric vehicles. *IEEE Trans Power Syst* 2015; 30(6): 3110–19.
- [8] Wang M, Mu Y, Jia H, Wu J, Yu X, Qi Y. Active power regulation for large-scale wind farms through an efficient power plant model of electric vehicles. *Appl Energy* 2017; 185: 1673–83.